

Periodic Modulations of Optical Tweezers Near Solid-State Membranes

Gautam V. Soni, Magnus P. Jonsson, and Cees Dekker*

Optical tweezers coupled to surfaces and thin solid-state membranes are very useful in a wide range of nanophotonics applications and open up new ways of measuring surface adhesion and molecular forces. A recent example is the coupling of optical tweezers to solid-state nanopore sensors for accurate control and biophysical investigation of single DNA molecules. Such membrane-integrated optical traps do, however, show a variety of optical effects that are not well understood. A major limitation in these experiments comes from periodic modulations of the bead position from the trapping plane when the optical trap is axially moved towards the membrane. While previously considered detection artifacts, it is shown here that these modulations correspond to real movements of the optical trap position that results from interference between the incident trapping laser and reflections from the thin solid-state membrane. An experimental study of these oscillations is presented, as well as optical simulations based on the finite-difference time-domain method, providing insight into the underlying interference phenomenon. Finally, an alternate measurement geometry is presented that eliminates these oscillations, specifically useful for performing optical-trap-coupled nanopore force spectroscopy.

Since its invention nearly 35 years ago optical tweezers have become a ubiquitous technique in micro- and nano-scale biophysics, in the fields of colloidal chemistry, surface analysis and single-molecule manipulation.^[1–3] Optical tweezers have also been coupled with other single-molecule techniques^[4–6] and solid-state devices^[7–9] in a variety of complex experimental geometries.^[10–14] By trapping microspheres tethered near silicon nanomembranes^[15] and nanowires,^[16] optical tweezers are used as an irreplaceable tool for manipulating solid-state membranes with high precision in a large variety

of fields such as fast-flexible electronics, optoelectronics, nanophotonics^[17] and more recently in biosensing. All these applications have in common that a microsphere is trapped near a free-standing thin membrane for manipulating either the membranes themselves or for manipulation of bead-tethered single molecules near the solid-state membrane. This common approach results in a variety of novel optical effects that are caused by the proximity of a solid-state membrane near the optical trap.

One of the recent advances in this field is the coupling of optical-tweezers-based force probes with solid-state nanopores. Here, an optical-tweezers force probe is used to measure electrophoretic forces on a biomolecule that is inserted into a nanopore drilled in a thin solid-state membrane.^[18–22] Interestingly large periodic fluctuations in the measured trapped-bead position have been observed when the trapped bead is axially moved towards the thin membrane.^[19,21] In these reports, the position of the bead in trap was measured using a co-aligned low-power detection laser. The oscillatory behavior, seen up to a distance of several microns from the membrane, was attributed to interference effects in the

G. V. Soni,^[+] M. P. Jonsson,^[+] Prof. C. Dekker
Delft University of Technology
Faculty of Applied Sciences
Kavli Institute of NanoScience
Department of Bionanoscience
Lorentzweg 1, 2628 CJ Delft, The Netherlands
E-mail: c.dekker@tudelft.nl

[+] These authors contributed equally to this work.



DOI: 10.1002/sml.201201875

detection path resulting from superposition of detection-laser light back scattered from the bead and the membrane. These oscillations near nanometer-thin membranes have limited the use and spread of these applications, and significant design changes have been employed by researchers to attempt to circumvent these effects and the errors that they introduce in the measurements.^[21]

In this paper, we present a detailed description of the origins of this oscillatory behavior and show that it is not a detection artifact, but a real modulation of the axial height of the trapping plane when the trap is approaching a thin membrane. We conclude that it is a generic phenomenon associated with the operation of optical tweezers near a thin solid state membrane. We show that as the optical trap axially moves towards the solid-state membrane, the laser light reflected off the free standing membrane creates a moving fringe pattern over the trap which periodically oscillates the position of the laser trapping plane. To gain a better understanding, we measure these effects under a variety of experimental conditions and build a computational model of the experimental geometry using the finite-difference time-domain method. We find that our model reproduces all the effects seen in the experiment remarkably well. Finally, we show an alternative experimental geometry to combine optical traps to nanopore measurements that eliminates the oscillatory effects.

Figure 1a shows a schematic of the experimental geometry. An optical tweezers setup is integrated with a nanopore setup,^[20,23] see the Experimental Section. Briefly, a streptavidin-coated 2 μm diameter polystyrene bead is trapped with optical tweezers, near a silicon nitride membrane. For the measurements reported here, a free-standing membrane with 20 nm LPCVD silicon nitride, 100 nm thermally grown silicon oxide and 500 nm LPCVD silicon nitride was used. In a typical experiment, a membrane is mounted on a piezo stage with nanometer resolution and is brought above the stationary optical trap, allowing control of the membrane-trap distance. In the absence of any membrane, a bead is trapped at the trapping plane of the optical tweezers (marked as ‘Trapping plane (no membrane)’ in Figure 1a). While monitoring the position of the trapped bead, the solid-state membrane is slowly brought down towards the bead, until it contacts and starts to push against it. The position of the new trapping plane, in the presence of the membrane (marked as ‘Trapping plane (with membrane)’ in Figure 1a), is estimated by measuring the offset in bead’s Z height (ΔZ_{ht}) as a function of bead-membrane distance (D_{bm}), see Figure 1a.

In earlier experiments, the axial position of the trapped bead was measured using a quadrant photo detector and a low-power 635 nm red laser that was co-aligned with a 1064 nm trapping infrared laser.^[19] Because both the trapping and detection lasers may individually result in interference effects, we reconfigured our setup to measure the trapped bead position using a laser-independent video-imaging method (see the Experimental Section). For bead-position detection, the sample is illuminated through the membrane with light from a high-power LED and the trapped bead is imaged on a CCD camera. From the diffraction rings of bead images, we estimate the center (X,Y) position

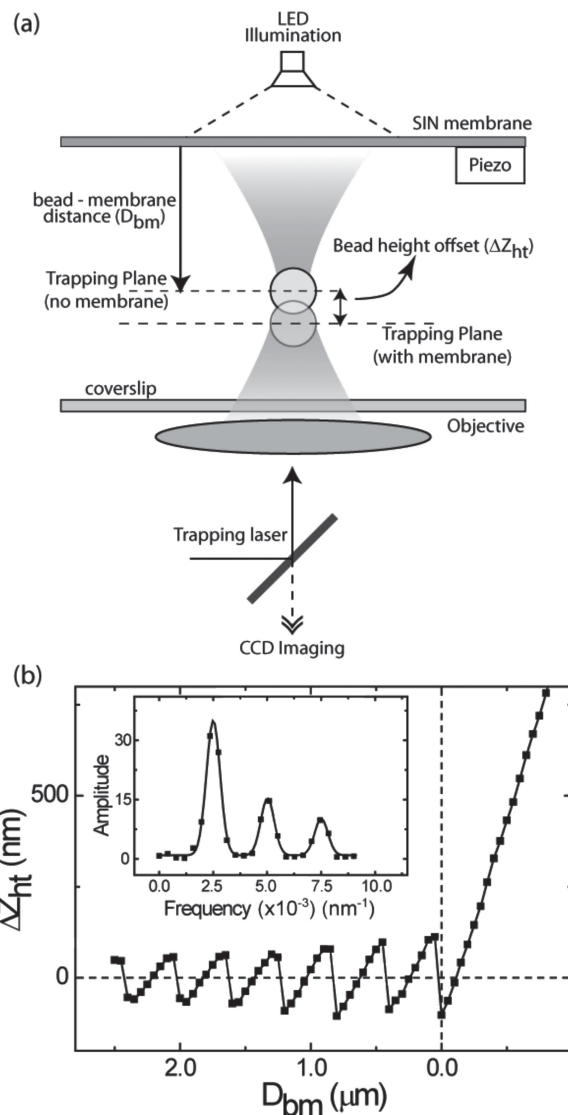


Figure 1. (a) Schematic of the experimental geometry. In the absence of any membrane, the bead is trapped in the optical trap at the Trapping Plane (no membrane). In the presence of a membrane, an axial offset appears in the trapped bead position, is shown as ΔZ_{ht} . LED illumination is used to image the trapped bead onto a CCD camera. (b) Bead height offset (ΔZ_{ht}) versus the bead-membrane distance (D_{bm}) upon moving the membrane towards the trapped bead using a piezo stage., is plotted along the x-axis. A sawtooth periodic modulation of (ΔZ_{ht}) is observed. In all figures D_{bm} is set to zero when the approaching membrane contacts the trapped bead. Inset: shows the Fourier spectrum of the bead oscillations. Peaks positions and standard errors corresponding to the fundamental frequency (0.00250 nm^{-1}) and its even (0.00502 nm^{-1}) and odd (0.00751 nm^{-1}) harmonics are estimated by Gaussian fits (solid line).

as well as the axial height of the bead with nanometer accuracy, by comparing them to a pre-measured look-up table, using a video tracking algorithm similar to that used in magnetic-tweezers measurements.^[24] The video-tracking-based scheme allows for measurement of the effect of an approaching solid-state membrane on the axial position of an optically trapped bead, independent of any detection laser.

Figure 1b shows the measured offset in the bead height (ΔZ_{ht}) from the trapping plane as a thin free-standing membrane is brought closer to the trapped bead (D_{bm}) using a piezo stage. The bead position is found to change periodically in a saw-tooth fashion as the membrane moves towards the trapped bead. Once the membrane contacts the bead surface ($D_{bm} = 0$), it pushes against the bead. The amplitude of the axial oscillations of the bead significantly increases as the membrane gets closer, reaching amplitudes of up to hundreds of nanometer before finally coming into contact with membrane. To facilitate comparison of the results at different experimental conditions, we will present the oscillation amplitude at $D_{bm} = 1.5 \mu\text{m}$ as the characteristic value; here, $135 \pm 5 \text{ nm}$. We find that the bead oscillates in a sawtooth-like fashion and indeed in its Fourier spectra, we find peaks at the fundamental frequency and both its even and odd harmonics (see inset of Figure 1b). The period of the oscillations is measured by fitting these peaks to Gaussian profiles. Interestingly, we find an oscillation period p of $400.0 \pm 1.7 \text{ nm}$ (errors shown are the standard error in peak center estimation of the Gaussian fit), which equals half the wavelength of the 1064 nm laser light in the medium (see below for more details). This suggests that the behavior is related to interference effects of the trapping laser.

To further investigate the source of the oscillations, we measured changes in the height of a trapped bead under different experimental conditions. **Figure 2** shows a comparison of the traces of bead z-height offset as the nanopore membrane is approached towards the trapped bead with different values for the membrane approach speed, trapping laser power, wavelengths of LED illumination, and thickness of

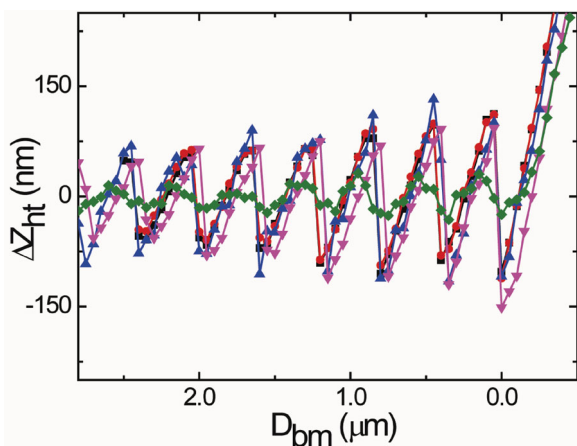


Figure 2. Trapped bead height (ΔZ_{ht}) versus bead-membrane distance (D_{bm}) under different experimental conditions. All measurements are done at standard parameters (except mentioned otherwise) of membrane approach speed of 100 nm/s, trap laser power of 2.5 W, green LED illumination and membrane thickness of 620 nm (Black squares, also plotted in Figure 1b). For the rest of the traces, one parameter was changed at a time: approach speed is reduced to half (50 nm/s; red circles), trapping laser power (as measured in front of the laser module) was reduced to 100 mW (blue triangles); illumination LED light was changed to white light (magenta inverted triangles); and the membrane was replaced by a 20 nm-thin free-standing silicon nitride membrane (green diamonds).

the free-standing solid-state membrane. First, we measure the effect of membrane approach speed on the ΔZ_{ht} oscillations. By reducing the speed of the membrane approach by a factor of 2 (red circles), the oscillations remain indistinguishable from that measured in Figure 1b (plotted as black squares in Figure 2). The oscillation period is $398.4 \pm 2.1 \text{ nm}$ and the amplitude is $127 \pm 5 \text{ nm}$ at $D_{bm} = 1.5 \mu\text{m}$. To remove any possibility that the illumination light affects the oscillations, we performed experiments with different illumination light sources. In Figure 2 we compare oscillations in the trapped-bead position when beads are imaged using green (532 nm) LED illumination and compare it to white LED illumination. The bead oscillations were found to be similar also under these conditions (Figure 2, downward magenta triangles). The period and amplitude of the oscillations at $1.5 \mu\text{m}$ distance from the membrane were measured as $398.4 \pm 3.5 \text{ nm}$ and $143 \pm 5 \text{ nm}$, respectively. Furthermore, we investigate the effect of laser power on the oscillations. Reducing the laser power by a factor of 25 (from 2.5 W to 100 mW) again did not affect the magnitude and period of the oscillations, as shown in Figure 2 (blue upward triangles). Since the trap is now weaker, the noise in the bead ΔZ_{ht} traces is higher. We find that the period of the oscillations and the amplitude (at $D_{bm} = 1.5 \mu\text{m}$ from the membrane) to be $401.6 \pm 5.6 \text{ nm}$ and $183 \pm 5 \text{ nm}$, respectively. Finally, to investigate a possible influence of the membrane thickness, we performed experiments with 20 nm-thick free-standing silicon nitride membranes (as opposed to the thickness of 620 nm in Figure 1b). As shown in Figure 2 (green diamonds), the oscillations are again present with a period of $395.2 \pm 4.5 \text{ nm}$, but their amplitude at $1.5 \mu\text{m}$ from the membrane is reduced to around $39 \pm 5 \text{ nm}$.

Based on the results above, we propose the following model for the saw-tooth oscillations of the trapped bead position in the presence of an approaching membrane. In the absence of any reflective surface, the focal spot (the trap center) results in a Gaussian intensity profile along the axial direction. In the presence of the membrane, the light that is reflected from the membrane interferes with the incoming laser light, forming intensity fringes along the axial direction.^[12] The fringe closest to the trap center axially offsets the position of the highest intensity spot (the trap center). The trapped bead follows this position of highest intensity, i.e., *not* the original laser focus position. As the membrane is translated towards the trapped bead, the intensity fringes move across the trap center, continuously offsetting the trap center until the next fringe moves in. Periodically, the next fringe creates a new maximum to which the bead jumps, which results in a saw-tooth oscillatory modulation of the bead position. Note that the change in propagation length of the reflected light is twice the distance travelled by the membrane. Hence, based on this physical picture, we expect the period of the oscillations to be equal to half the trapping-laser wavelength in the medium. This gives $p = \lambda/2n = 400 \text{ nm}$, where λ is the wavelength of the trapping laser in vacuum ($\lambda = 1064 \text{ nm}$) and n is the index of refraction of the medium ($n = 1.33$). This is in excellent agreement with the oscillation period measured in all experiments.

For a better understanding of the observed oscillations, we modeled an optical trap near a thin membrane using the finite-difference time-domain (FDTD) method (Lumerical

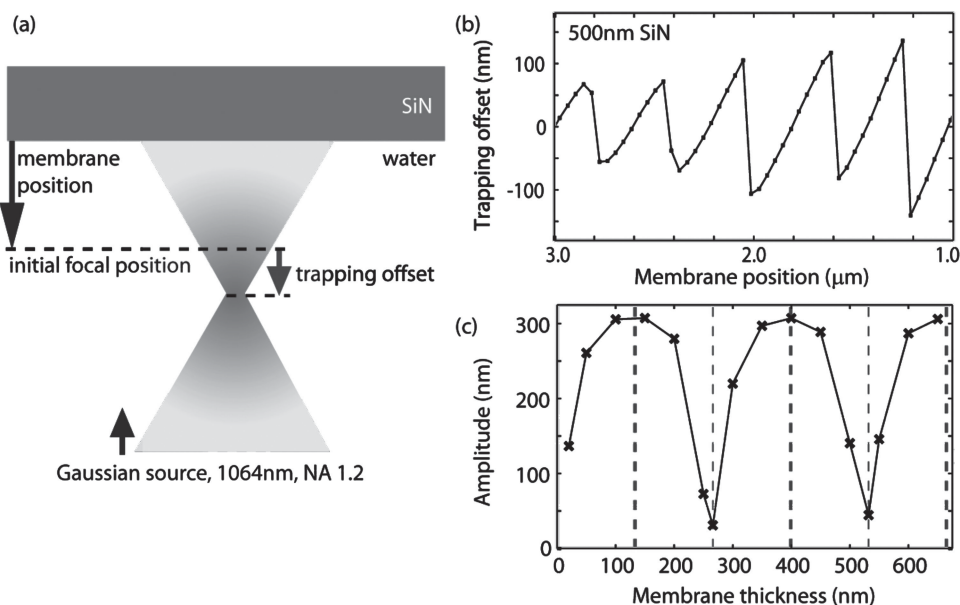


Figure 3. FDTD simulations. (a) Schematic illustration of the simulation setup. (b) Simulated results for the trapping offset versus distance to a 500 nm SiN membrane. (c) Trap oscillation amplitude as a function of membrane thickness. The crosses correspond to simulated values and the solid line is a guide to the eye. The thick and thin dashed lines mark the positions of predicted maxima and minima, respectively.

Solutions, Inc., Canada). A Gaussian thin lens source with an NA of 1.2 and a wavelength of 1064 nm was used to model the laser source. The solid-state membrane was modeled as a 500 nm thick slab of silicon nitride using a refractive index of 2 (see **Figure 3a**). The surrounding environment was set to a refractive index of 1.33 to match the experimental conditions. The position of the trapping plane for a given geometry was evaluated as the position of highest electric field intensity along the propagation direction (z-axis) after fitting the simulation results to a polynomial. We define the zero value of the modeled trap position as the plane of the initial laser focus (Figure 3a), as obtained from a simulation without a membrane in the simulation region. Figure 3b shows the simulated offset in position of the trapping plane for different distances between the initial laser focus and the membrane. It is evident that the simulations reproduce the saw-tooth oscillatory behavior that was observed experimentally. The oscillation period is found to be 398 ± 7 nm, which is in agreement with the experimental value of about 400 nm. Also the amplitude of 140 nm at the membrane distance of 2.5 μm (corresponding to 1.5 μm distance from the membrane for a 2 μm diameter bead) is of the same order as the experimentally measured values. Note that, in contrast to the experimental situation, no bead was used in the simulations. The simulations further support our hypothesis that the trap oscillations are a result from interference between the incident trapping laser and laser light reflected by the thin membrane, whereas possible influence of the trapped bead plays a minor role.

Next we used the simulations to investigate the dependence of the oscillations on membrane thickness. For each membrane thickness, the amplitude of the oscillations was measured at 2.5 μm from the simulated membrane, corresponding to 1.5 μm distance between a membrane and the

surface of a 2 μm diameter bead, as used in the experiments. As shown in Figure 3c there is a strong dependence of the oscillation amplitude on membrane thickness. The curve is not monotonic, but contains several maxima and minima. This can be understood by considering that a thin solid-state membrane has two closely spaced reflecting surfaces. Reflections from these two interfaces will interfere constructively or destructively depending on the membrane thickness. Hence, the membrane thickness will influence the total fraction of light that is reflected by the membrane and in turn, will determine the amount of light that can interfere with the initial optical trap. The phase difference, Δp , between light reflected from the two interfaces (at normal incidence angle) is given by, $\Delta p = \frac{2\pi}{\lambda} 2tn - \pi$, where λ is the wavelength of the laser in vacuum and n and t are the refractive index and the thickness of the membrane, respectively. From this relation we calculate the thicknesses that correspond to constructive ($\Delta p = 0, 2\pi, \dots$, thick dashed lines in Figure 3c) and destructive ($\Delta p = \pi, 3\pi, \dots$, thin dashed lines in Figure 3c) interference and they perfectly overlap with the maxima and minima obtained from the FDTD simulations. This explains the experimental observation of strongly different oscillation amplitude between thin (20 nm) and thick (620 nm) membranes.

From this understanding of the behavior of an optical trap near a solid-state membrane, it is clear that the oscillations may be reduced, yet not fully eliminated by a very precise control of the membrane thickness. However, for many experiments, changing the membrane thickness is impractical, because it influences other experimental conditions. In the example of optical tweezers coupled to a nanopore sensor setup, this includes the electrical noise, structural stability and the detection sensitivity.^[25,26] With this in mind, we present an alternate, much simpler and more versatile

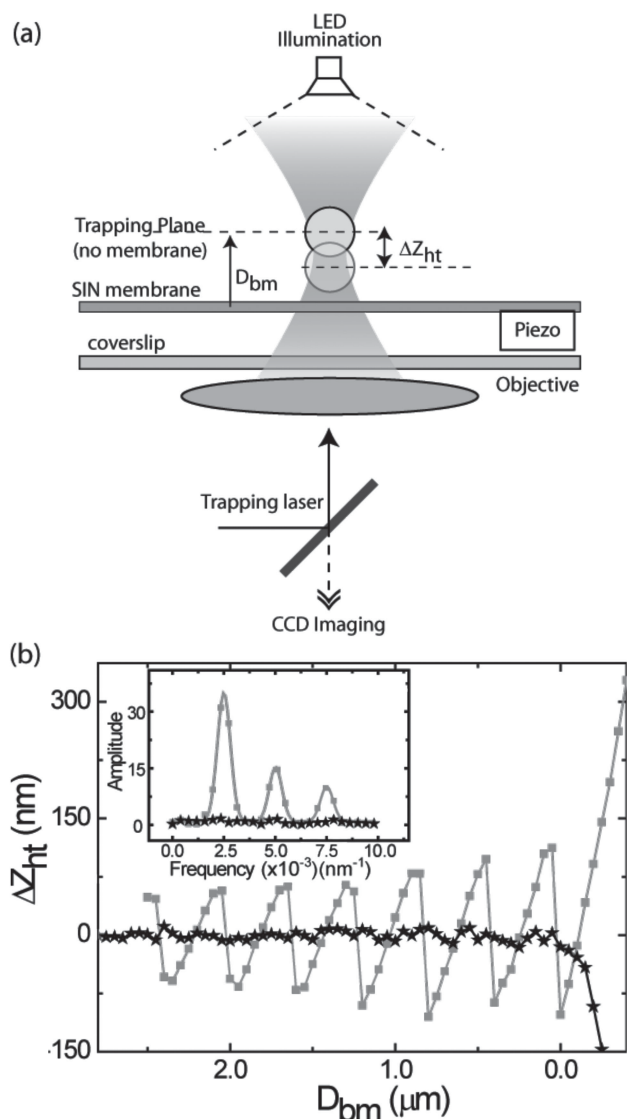


Figure 4. Alternate experimental geometry to remove trap oscillations. The laser passes through the solid-state membrane and traps the beads on the far side of membrane. This geometry eliminates all reflection-based effects on the optical trap, and bead oscillations during a membrane approach are removed. (b) Comparison of offset in trapped bead height when a 620 nm thick membrane is approached, when the bead is trapped below (gray square; same as Figure 1b) and above (solid stars) the nanopore membrane. Inset: Fourier spectrum of approach trace for bead trapped above (solid stars) and below (gray squares and line; same as Figure 1b inset) the membrane is plotted.

experimental geometry that removes the axial oscillations of the optical trap center upon an approaching free-standing membrane. This alternate experimental geometry is schematically shown in **Figure 4a**. We inverted the experimental geometry, where now the trapping laser passes through the thin solid-state membrane and traps the bead on the other side of the membrane. In this geometry, there are no reflective surfaces above the trap and thus all the reflection-based effects on the trap are removed, apart from reflections of the trapped bead itself which constitutes a much smaller effect.^[27] Figure 4b (solid stars) shows the experimental ΔZ_{ht}

traces where the bead is trapped above the membrane and the membrane is moved upwards to finally contact the bead. For comparison, the membrane approach trace of Figure 1b, where the bead is trapped under the membrane, is also plotted (gray squares). In inset to Figure 4b, we show that the Fourier spectrum of the approach trace for bead trapped above-the-membrane (solid stars) is flat and featureless. As is clear from the trace in Figure 4b, the reflection-based oscillations that were previously seen are removed. Any possible effects due to reflections of the bead^[27] appear to be well within the thermal fluctuations of the measured bead position. This new geometry alleviates the oscillations and is fully compatible with all the conceived optical-trap-coupled nanopores-based experiments. The only minor disadvantage is that trapping beads on the far-side of the membrane will result in $\sim 10\%$ lower laser power due to reflection and absorption by the membrane.

In conclusion, we present a detailed description of the optical effects when working with optical tweezers near free-standing solid-state membranes. The origin of the observed oscillatory signal in experiments with nanopore-coupled optical tweezers instruments was revealed and described. We find saw-tooth oscillations that are due to reflections of the trapping laser from the solid-state free standing membrane that interferes with and modifies the incident intensity profile of the focused laser trap, resulting in an axially re-positioned trap center. Movement of the membrane interface towards the bead causes the axial position of the trap center to oscillate in a saw-tooth manner. Our model is supported by computer simulations that reproduce all the salient features of these experimentally observed oscillatory effects. For the conventional geometry, the presented description of the oscillations can be helpful in determining the distance of the trapped bead from the nanopore membrane. Finally, we describe an alternate experimental geometry, where the laser passes through the thin membrane and the bead is trapped on the far side of the membrane. This geometry removes effects of any laser reflections from the membrane on trap position. We demonstrate that this new experimental geometry removes the observed errors in force measurements in a nanopore using optical tweezers as a force transducer. Combination of optical tweezers with nanometer thick membranes is used in a variety of nanophotonics and biosensing applications. These experiments and devices are limited in their applications due the inherent effects of reflections on the optical tweezers. Our description and remedy of this effect should be useful for a broad range of applications in surface biophysics, colloidal chemistry and single-molecule nanopore biosensing.

Experimental Section

Optical Tweezers: Free standing nanopore membranes are fabricated^[28,29] using standard photolithography and e-beam lithography methods. These solid-state membranes were mounted on glass coverslips in a custom-made flowcell consisting of polydimethyl siloxane (PDMS) and polyether ether ketone (PEEK)

components permitting fluid access to both sides of the membrane^[19] as well as optical measurements. This flowcell is mounted on a 1.2NA (60×) water immersion objective (Olympus), through which both the optical trapping as well as optical imaging is achieved. The optical tweezers were constructed as described previously.^[19] Briefly, a 1064 nm laser beam (COMPASS 1065–4000M, Coherent Inc.) was expanded using a beam expander and focused to a diffraction limited spot using the objective. The working distance of the objective (0.28 mm) allows for trapping of beads both below and above the nanopore membrane. Collimated light from high power green/white light LED was used for illumination of sample and was imaged on a CMOS camera (MC1362, Mikrotron). The x,y and z-position of a trapped bead was estimated with nanometer accuracy by comparing the defocusing rings of the bead with previously measured look-up-table generated by defocusing the bead immobilized on surface. The 3D tracking routine is described in detail, elsewhere.^[24]

FDTD simulations: The FDTD simulations were performed using the commercial software Lumerical FDTD Solutions (Lumerical Solutions, Inc., Canada). A Gaussian thin lens source with an NA of 1.2 and a wavelength of 1064 nm was used to model the laser source. No further corrections were made for aberrations resulting from tight focusing of a laser beam within the flow cell. A silicon nitride membrane of given thickness was modeled using a refractive index of 2. The surrounding environment was set to a refractive index of 1.33. The simulations were performed in a region of 15 μm × 15 μm × 8 μm, where the letter is the direction along the light propagation. Conformal meshing was employed and extra fine mesh boxes were added close to the focal plane and around the moving membrane (with at least 10 mesh cells over the membrane for any given thickness). To reduce the computational time we used anti-symmetric (parallel with the source polarization) and symmetric (orthogonal to the source polarization) boundary conditions for the two axes orthogonal to the source propagation direction. Perfectly match layers were used to absorb the fields and avoid reflection from the boundaries of the simulation region.

Acknowledgements

We thank X.J.A Janssen for help with fabrication of silicon nitride membranes and J.W.J. Kerssemakers for discussions on video imaging methods. G.V.S and C.D. acknowledge support from ERC-2009-AdG Grant NANOforBIO and M.P.J. acknowledges support from the Wenner-Gren foundations.

- [1] A. Ashkin, *Proc. Natl. Acad. Sci. USA* **1997**, *94*, 4853.
- [2] A. Ashkin, J. M. Dziedzic, *Science* **1975**, *187*, 1073.
- [3] J. R. Moffitt, Y. R. Chemla, S. B. Smith, C. Bustamante, *Annu. Rev. Biochem.* **2008**, *77*, 205.
- [4] R. R. Brau, P. B. Tarsa, J. M. Ferrer, P. Lee, M. J. Lang, *Biophys. J.* **2006**, *91*, 1069.
- [5] F. Qian, S. Ermilov, D. Murdock, W. E. Brownell, B. Anvari, *Rev. Sci. Instrum.* **2004**, *75*, 2937.
- [6] A. Candelli, G. J. Wuite, E. J. Peterman, *Phys. Chem. Chem. Phys.* **2011**, *13*, 7263.
- [7] P. Gross, G. Farge, E. J. Peterman, G. J. Wuite, *Methods Enzymol.* **2010**, *475*, 427.
- [8] J. H. Huisstede, V. Subramaniam, M. L. Bennink, *Microsc. Res. Tech.* **2007**, *70*, 26.
- [9] D. C. Appleyard, M. J. Lang, *Lab Chip* **2007**, *7*, 1837.
- [10] F. Difato, M. Dal Maschio, E. Marconi, G. Ronzitti, A. Maccione, T. Fellin, L. Berdondini, E. Chierigatti, F. Benfenati, A. Blau, *J. Biomed. Opt.* **2011**, *16*, 051306.
- [11] B. H. Liu, L. J. Yang, Y. Wang, *Opt. Express* **2011**, *19*, 3703.
- [12] A. Jonass, P. Zemanek, E. L. Florin, *Opt. Lett.* **2001**, *26*, 1466.
- [13] M. Veiga-Gutierrez, M. Woerdemann, E. Prasetyanto, C. Denz, L. De Cola, *Adv. Mater.* **2012**, *24*, 5198.
- [14] M. Woerdemann, S. Glasener, F. Horner, A. Devaux, L. De Cola, C. Denz, *Adv. Mater.* **2010**, *22*, 4176.
- [15] S. M. Oehlein, J. R. Sanchez-Perez, R. B. Jacobson, F. S. Flack, R. J. Kershner, M. G. Lagally, *Nanoscale Res. Lett.* **2011**, *6*, 507.
- [16] P. J. Pauzauskie, A. Radenovic, E. Trepagnier, H. Shroff, P. D. Yang, J. Liphardt, *Nat. Mater.* **2006**, *5*, 97.
- [17] F. Cavallo, M. G. Lagally, *Soft Matter* **2010**, *6*, 439.
- [18] C. Dekker, *Nat. Nanotechnol.* **2007**, *2*, 209.
- [19] U. F. Keyser, J. van der Does, C. Dekker, N. H. Dekker, *Rev. Sci. Instrum.* **2006**, *77*, 105105.
- [20] A. R. Hall, S. van Dorp, S. G. Lemay, C. Dekker, *Nano Lett.* **2009**, *9*, 4441.
- [21] A. Sischka, C. Kleimann, W. Hachmann, M. M. Schafer, I. Seuffert, K. Tonsing, D. Anselmetti, *Rev. Sci. Instrum.* **2008**, *79*, 063702.
- [22] E. H. Trepagnier, A. Radenovic, D. Sivak, P. Geissler, J. Liphardt, *Nano Lett.* **2007**, *7*, 2824.
- [23] U. F. Keyser, B. N. Koeleman, S. Van Dorp, D. Krapf, R. M. M. Smeets, S. G. Lemay, N. H. Dekker, C. Dekker, *Nat. Phys.* **2006**, *2*, 473.
- [24] M. T. van Loenhout, J. W. Kerssemakers, I. De Vlaminck, C. Dekker, *Biophys. J.* **2012**, *102*, 2362.
- [25] R. M. Smeets, U. F. Keyser, N. H. Dekker, C. Dekker, *Proc. Natl. Acad. Sci. USA* **2008**, *105*, 417.
- [26] M. Wanunu, T. Dadoosh, V. Ray, J. M. Jin, L. McReynolds, M. Drndic, *Nat. Nanotechnol.* **2010**, *5*, 807.
- [27] K. C. Neuman, E. A. Abbondanzieri, S. M. Block, *Opt. Lett.* **2005**, *30*, 1318.
- [28] M. van den Hout, A. R. Hall, M. Y. Wu, H. W. Zandbergen, C. Dekker, N. H. Dekker, *Nanotechnology* **2010**, *21*, 115304.
- [29] A. J. Storm, J. H. Chen, X. S. Ling, H. W. Zandbergen, C. Dekker, *Nat. Mater.* **2003**, *2*, 537.

Received: August 2, 2012
Published online: